Available online at www.sciencedirect.com
ScienceDirect
Catalysis Today 129 (2007) 247–255
CATALYSIS TODAY
www.elsevier.com/locate/cattod

The ''Direct–Indirect'' model: An alternative kinetic approach in heterogeneous photocatalysis based on the degree of interaction of dissolved pollutant species with the semiconductor surface

Damián Monllor-Satoca [a], Roberto Gómez [a], Manuel González-Hidalgo [b], Pedro Salvador [a,b,1,*]

[a] *Departament de Química Física and Institut Universitari d'Electroquímica, Universitat d'Alacant, E-03080 Alacant, Spain*
[b] *Departament de Matemàtiques i Informàtica, Universitat de les Illes Balears, E-07071 Palma de Mallorca, Spain*

Available online 10 September 2007

Abstract

The analysis of photocatalyst kinetics concerning degradation of water dissolved pollutants with TiO_2 suspensions has been built on for years in a robotic way on the basis of the ''Langmuir–Hinshelwood'' (L–H) model. According to the L–H model the reaction rate is described by the equation: rate = $k_{LH}K_L[M]/(1 + K_L[M])$, where K_L is the Langmuir adsorption constant, k_{LH} the apparent Langmuir rate constant and $[M]$ is the reactant concentration. Even in cases where 1/rate versus 1/$[M]$ plots are apparently linear, as predicts the previous equation, it is frequently found that K_L depends on the illumination flux, Φ, which contradicts the L–H model premise that equilibrated adsorption/desorption of reactants is maintained under illumination. Moreover, the L–H model does not define the k_{LH} dependence on Φ, so that by itself is unable to predict any existing relationship between Φ and the reaction rate. Here we describe in detail an alternative kinetic approach, the ''Direct–Indirect'' (D–I) model, which is based on the degree of electronic interaction of the semiconductor surface with dissolved reactant molecules. The D–I model introduces the systematic use of fundamental concepts like direct, indirect, adiabatic and inelastic interfacial transfer of charge as basic tools, giving a physical meaning to the involved kinetic parameters. Moreover, it is shown to be able to predict the functional dependence of the photooxidation rate on the experimental parameters (photon flux and pollutant concentration), distinguishing between strong (specific adsorption) and weak semiconductor–reactant interaction (absence of specific adsorption). The general believe that $OH^\bullet$ radicals, either TiO_2-adsorbed or free, photogenerated from OH^- groups adsorbed on terminal Ti atoms, behave as active species in interfacial oxidation reactions is disregarded by the D–I model, as adsorbed OH^- groups cannot be photooxidized with valence band holes.

Keywords: Photocatalysis; TiO_2-substrate interaction; Kinetic models; Rate equations: Primary reactions

1. Introduction

The scientific and technological interest in the application of heterogeneous photocatalysis with suspensions of TiO_2 nanoparticles has grown exponentially during the last two decades. About 95 documents concerning TiO_2 photocatalysis were published in 1985, 247 in 1995 and 2032 in 2005; in total about 14,000 documents during the period 1985–2006 [1]. In spite of this interest, detailed mechanisms of the photocatalytic processes, and specially those concerning the initial steps involved in the reaction of photogenerated electrons and holes with dissolved reactants, are far to be clear. It is well established that interfacial transfer of conduction band electrons to dissolved O_2, which acts generally as primary electrolyte electron acceptor, is the rate determining step of the whole photocatalytic reaction [2,3]. With respect to photooxidation reactions, a first source of debate comes from whether delocalized (free), photogenerated valence band holes (h_f^+) react directly with the organic substrate via a direct transfer (DT) mechanism, or photooxidation occurs via an indirect transfer (IT) mechanism with intervention of photogenerated $OH^\bullet$ radicals (surface trapped holes, h_s^+) [4]. Both processes can be correlated with the well known outer sphere (IT) and inner sphere (DT) electron transfer mechanisms. Although h_f^+ and $OH^\bullet$ mediated pathways are different processes, both lead to a similar distribution of photooxidized products, which

* Corresponding author at: Departament de Ciències Matemàtiques i Informàtica, Universitat de les Illes Balears, E-07071 Palma de Mallorca, Spain. Tel.: +34 971 172962; fax: +34 971 173003.
E-mail address: dmipss9@uib.es (P. Salvador).
[1] On leave from the Instituto de Catálisis y Petroleoquímica, CSIC.

0920-5861/$ – see front matter © 2007 Elsevier B.V. All rights reserved.
doi:10.1016/j.cattod.2007.08.002

makes their distinction difficult. This is the reason why the nature of the interfacial hole transfer mechanism, either direct or indirect, is in many cases object of controversy [5]. Another source of debate is related to the localization of the photooxidation process. Adsorption of dissolved organic molecules (reactants) to the TiO_2 surface is often believed to be a prerequisite for photooxidation. However, some authors suggest that in the case of IT, adsorption is not required, as far as photogenerated $OH^{\bullet}$ radicals can diffuse into the solution to react with organic molecules [4,6]. Whether a prerequisite or not, the existence or absence of specific adsorption seems to be critical [5].

Numerous researchers have reported that the photooxidation rate follows a classical Langmuir–Hinshelwood (L–H) mechanism [4,7–10], assuming implicitly adsorption/desorption equilibrium of reactants (Langmuir isotherm), not only in the dark but also under illumination [9]. The L–H model establishes that the photooxidation rate, v_{ox}, depends on the concentration of reactants, $[RH_2]_{aq}$, according to the relationship $v_{ox} = k_{LH}K_L[RH_2]_{aq}/(1 + K_L[RH_2]_{aq})$, where k_{LH} is the apparent L–H rate constant and K_L is the photon-flux-independent Langmuir equilibrium adsorption/desorption constant. Alternatively, a pseudo-steady-state analysis has been proposed for the case that adsorption/desorption equilibrium is broken under illumination [9].

The application of the L–H model to the interpretation of kinetic data in heterogeneous photocatalysis has received the category of dogma for most authors [10]. One of the limitations of the LH model resides in its incapacity to define a relationship between v_{ox} and the illumination photon flux, Φ, unless the dependence of k_{LH} on Φ is known. The pseudo-steady-state approach of the LH model leads to the rate expression [10]:

$$v_{ox} = \frac{k_{abs}k_r\Phi[s][RH_2]_{aq}}{k_d + k_r[RH_2]_{aq}} \quad (1)$$

where $[s]$ is the concentration of oxidant active species (h_f^+, h_s^+), k_{abs} and k_d are the rate constants for generation and decay of photoactive species, respectively, and k_r is the rate constant for reaction of h_f^+ and/or h_s^+ species with $(RH_2)_{aq}$ dissolved organic molecules. However, Eq. (1) formally belongs to an Eley–Rideal (ER) type mechanism [10], and apparently predicts a linear dependence of v_{ox} on Φ and, therefore, a photon flux independent quantum yield. Eq. (1) can be reduced to the L–H equation by substituting $k_{abs}\Phi[s]$ for k_{LH} and $k_r/k_d = K_L$, although the physical sense of $k_r/k_d = K_L$ is entirely different from that given by the L–H kinetic treatment [11].

Trying to fill up the gaps existing in the understanding of the photocatalytic mechanisms, we have recently developed an alternative kinetic model which is based on the degree of interaction of dissolved organic species with the semiconductor surface [12–14]. This model, in the following the Direct–Indirect (D–I) model, introduces the concepts of direct, indirect, adiabatic and inelastic processes as basic tools for describing interfacial charge transfer. In the case of weak electronic interaction (absence of specific adsorption), the D–I model establishes that interfacial hole transfer takes place exclusively via an adiabatic IT mechanism involving surface trapped holes and dissolved reactant molecules within the electric double layer. In contrast, for the case of strong electronic interaction (specific adsorption), interfacial hole transfer takes place via a mixture of the IT and DT mechanism, IT prevailing at low enough Φ values while DT prevails at high enough Φ values [12]. Further, in contrast with the L–H model, the D–I model states explicitly the sequence of primary reactions occurring during the photocatalytic process and provides a comprehensible physical meaning to the kinetic constants appearing in the interfacial charge transfer reactions. This confers to the model the capability of predicting the influence that modifications of the photocatalyst, like doping, metal coating or specific adsorption of inorganic ions, exercise on its reactivity.

Here, we will go deeper into the understanding of these fundamental questions, emphasizing the main predictions of the D–I model with respect to the photooxidation quantum yield dependence on photon flux and reactant concentration.

2. About the nature of surface active photogenerated radical species: a misconception in TiO_2 photocatalysis

There exists a widespread consensus that a major photooxidizing role in TiO_2 photocatalysis is played by OH radicals photogenerated via trapping of valence band holes by water species adsorbed on terminal Ti atoms. However, this contradicts the fact, as deduced from UPS spectra of TiO_2(1 1 0) adsorbed water, that the top of the O:2p filled energy levels of adsorbed water species are far below the top of the TiO_2 valence band at the surface, which implicates that water molecules (and hydroxyl groups) adsorbed on terminal Ti atoms cannot be photooxidized with valence band holes [15,16]. Although these studies refer to a TiO_2(1 1 0) surface, the same conclusion should be valid for other crystal faces. In fact, the energy position of the electronic levels of the highest occupied molecular orbitals (HOMO) of adsorbed water molecules mainly depends on the interaction of 3d orbitals of terminal of Ti atoms with 1b1 H_2O orbitals [16], which should be scarcely influenced by crystal orientation. The consequence is that the only primary oxidant species active in photocatalytic reactions would be holes trapped at terminal O_s^{2-} intrinsic surface states ($O_s^{2-} + h_f^+ \rightarrow O_s^-(h_s^+)$) whose O:2p orbitals constitute the top of the valence band at the TiO_2 surface. The same is extensive to protonated O_s^{2-} terminal ions ($O_s^{2-} + H^+ \rightarrow (O^{2-} - H^+)_s$), which must be considered as lattice, surface hydroxyl groups (intrinsic surface states) having nothing to do with hydroxyl ions adsorbed on terminal Ti atoms (extrinsic surface states). Consequently, the assumed possible existence of free OH radicals in the aqueous solution as a result of the desorption of photogenerated, adsorbed OH radicals must be disregarded.

By employing time-resolved laser flash photolysis, Bahnemann et al. [17] have been able to detect two types of surface trapped holes: holes at deep traps, which are long-lived but non-reactive with specifically adsorbed species, and shallow traps in thermal equilibrium with top energy levels of the valence band and which reactivity is comparable to free holes. Deep traps of

Bahnemann et al. [17] could be identified with O_s^{2-} and/or $(O^{2-} - H^+)_s$ intrinsic surface states.

3. Direct versus indirect interfacial hole transfer

According to the D–I model, direct and indirect mechanisms play an essential role in interfacial hole transfer. On the one hand, DT of valence band free holes can occur either to $(RH_2)_{aq}$ dissolved species, in the absence of specific adsorption,

$$h_f^+ + (RH_2)_{aq} \xrightarrow{v_{DT,1}} (RH^\bullet)_{aq} + H_{aq}^+ \qquad (DT,1)$$

or to $(RH_2)_s$ specifically adsorbed species

$$h_f^+ + (RH_2)_s \xrightarrow{v_{DT,2}} (RH^\bullet)_s + H_{aq}^+ \qquad (DT,2)$$

On the other hand, IT of surface trapped holes also takes place to either $(RH_2)_{aq}$ dissolved species

$$h_s^+ + (RH_2)_{aq} \xrightarrow{v_{IT,1}} (RH^\bullet)_{aq} + H_{aq}^+ \qquad (IT,1)$$

or $(RH_2)_s$ surface-bound species

$$h_s^+ + (RH_2)_s \xrightarrow{v_{IT,2}} (RH^\bullet)_s + H_{aq}^+, \quad h_s^+ + (RH^\bullet)_s \xrightarrow{v'_{IT,2}} R + H_{aq}^+ \qquad (IT,2)$$

4. Adiabatic versus inelastic hole transfer

In the absence of specific adsorption, hole transfer to $(RH_2)_{aq}$ dissolved species takes place adiabatically, the transfer rate being defined by the Fluctuating Energy Level Model developed by Marcus [18] and applied by Gerischer to the semiconductor electrolyte interface [19,20]. This model predicts a hole transfer rate constant

$$k_{ox}^{adb} \propto \exp\left[\frac{-(E_{red} - E_s)^2}{4\lambda kT}\right] \qquad (2)$$

where E_s is the energy of surface trapped holes, h_s^+ (empty surface states) to which electrons are transferred adiabatically from filled energy levels of $(RH_2)_{aq}$ dissolved species, E_{red} the most probable energy for the occupied energy levels of $(RH_2)_{aq}$ species and λ is the reorganization energy (typical values of λ are between 0.5 and 1.0 eV). As shown in the energy diagram of Fig. 1, for DT, E_s represents the energy of valence band free holes ($E(h_f^+) \cong E_V$), while for IT, E_s is the energy of surface-trapped holes ($E_s \cong E(h_s^+)$). Because of the very positive value of E_V for TiO_2, except for highly reductant dissolved species, $(E_{red} - E_V)$ reaches quite high values (about 1.0 eV for the $H_3COH/H_2COH^\bullet$ redox couple by considering a $\lambda = 0.7$ eV) [21], which results in a extremely small value of k_{ox}^{adb} in Eq. (2) and, therefore, in a negligible probability of adiabatic DT. Adiabatic reactions in Fig. 1 are (DT,1) and (IT,1).

Under strong electronic interaction of dissolved reactant species with the semiconductor surface (specific adsorption in competition with that of water molecules), the hole transfer mechanism to $(RH_2)_s$ species is not adiabatic but inelastic, the Marcus–Gerischer model does not apply and the hole transfer

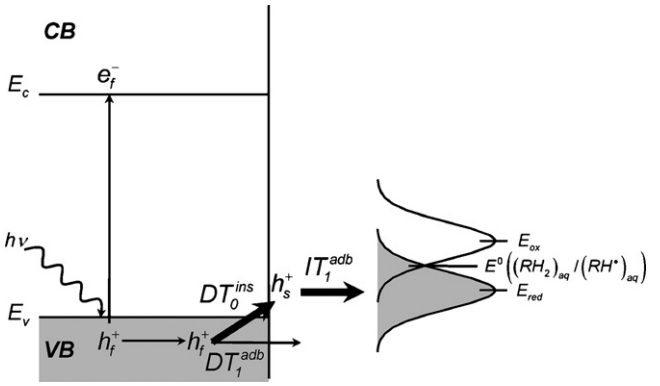

Fig. 1. Energy diagram showing TiO_2 and electrolyte energy levels according to the Marcus–Gerischer "Fluctuating Energy Level Model". The arrows indicate interfacial charge transfer reactions, either inelastic (vertical and/or leaned arrows), as is the case for direct interfacial transfer of h_f^+ valence band free holes to filled intrinsic bandgap surface states, to produce h_s^+ surface trapped holes (DT0), or adiabatic (horizontal arrows), as is the case for direct transfer of h_f^+ holes (DT,1) and indirect transfer of h_s^+ holes (IT,1) to filled energy levels of $(RH_2)_{aq}$ dissolved species. Rates are proportional to the arrow thickness, so that (IT,1) rate is higher than the (DT,1) rate, as the overlap with filled electrolyte levels is higher for h_s^+ than for h_f^+ holes.

rate constant is $k_{ox}^{ins} \propto \sigma\bar{c}$, where $\bar{c}$ is the thermal velocity of free holes and σ is the hole capture cross-section of filled surface states [22]. These can be either intrinsic, such as those associated to semiconductor surface atoms, or extrinsic, as correspond to electrolyte surface-bound species. In the latter case, σ depends on the degree of semiconductor–reactant electronic interaction. Since the activation energy term (exponential term) of Eq. (2) disappears in this case, v_{ox}^{ins} is generally higher than v_{ox}^{adb}, except for cases where $(E_{red} - E_s)$ is small enough. As shown in the energy diagram of Fig. 2, inelastic hole transfer reactions are (DT,2) and (IT,2), together with transfer of free holes to filled intrinsic surface states, which is defined by the rate v_0. Assuming that both h_s^+ and $(RH_2)_s$ species are immobile on the semiconductor surface, the redox

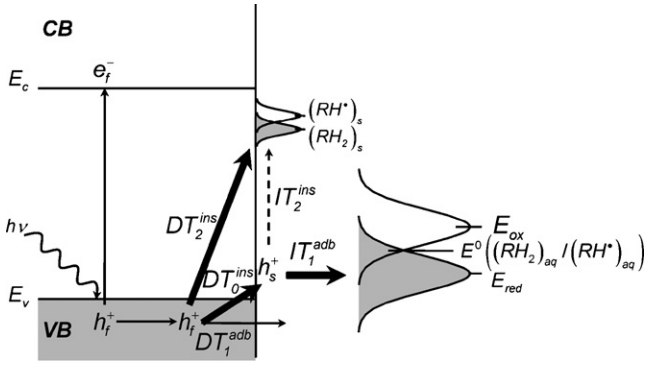

Fig. 2. Energy diagram showing interfacial hole transfer reactions. Direct hole transfers of h_f^+ holes to filled energy levels of intrinsic bandgap surface states, $(RH_2)_{aq}$ dissolved species or extrinsic bandgap states associated with $(RH_2)_s$ surface-bound species, are represented by DT_0^{ins}, DT_1^{adb} and DT_2^{ins}, respectively. Indirect transfer of h_s^+ holes to filled energy levels of either $(RH_2)_s$ surface-bound species or $(RH_2)_{aq}$ dissolved species is represented by their respective rates IT_2^{ins} and IT_1^{adb}. IT_2^{ins} mechanism is depicted by means of a dotted vertical arrow indicating that, in general, its rate can be considered to be negligible (see text).

Table 1
Main features of the D–I model

Substrate–TiO_2 interaction	Conventional kinetic model	Surface adsorptions sites	Prevailing D–I mechanisms
Specific adsorption	L–H	Terminal Ti_{is}^{IV}	DT, inelastic; IT, adiabatic
		Terminal O_s^{2-}	DT, inelastic
Absence of specific adsorption	E–R	–	IT, adiabatic

reaction (IT,2) would be very improbable, unless the surface density of $(RH_2)_s$ species is very high (near a mono-layer) so that the mean h_s^+–$(RH_2)_s$ distance is of the order of a few angstroms. In general $v_0 \gg v_{DT,1}$, $v_{DT,2} \gg v_{DT,1}$ and $v_{DT,2} \gg v_{IT,1}$, because of the existence of the exponential reorganization energy term for reactions (DT,1) and (IT,1).

In the case of specific adsorption, inelastic direct transfer (reaction (DT,2)) necessarily coexists with adiabatic indirect transfer (reaction (IT,1)). Only when $E_{red} \approx E_V$ (i.e., for very reductant $(RH_2)_{aq}$ species) it can be $v_{DT,2} \approx v_{DT,1}$. Moreover, it must be emphasized that indirect transfer is the only possible hole transfer mechanism in the absence of specific adsorption (IT,1).

Summing up, in the case of specific adsorption, DT should, in general, predominate on IT, although both mechanisms coexist. In contrast, in the absence of specific adsorption, IT is the only possible hole transfer mechanism. Moreover, because of the existence of an activation energy for IT, unless $E_{red} \approx E(h_s^+)$, it must be $k_{ox}^{ins} \ll k_{ox}^{adb}$, DT being more efficient than IT. Table 1 summarizes the main features of the D–I model. Note that neither the L–H model, which is based in the existence of specific adsorption, nor the E–R model, which is valid in the absence of specific adsorption, distinguishes between direct and indirect interfacial charge transfer [4]. Moreover, the photooxidation reactions involving surface-bound OH radicals as active species are not taken into account by the D–I model, as their existence is questionable (see Section 2).

5. Kinetic implications of DT and IT mechanisms: the photooxidation quantum yield dependence on photon flux and substrate concentration

5.1. The IT mechanism

The following primary interfacial reactions, which are described schematically in Fig. 3, are taken into account [12]:

Charge-carrier generation

$$TiO_2 + h\nu \xrightarrow{v_0'} h_f^+ + e_f^-, \quad v_0' = k_0'\Phi$$

Charge-carrier trapping

$$h_f^+ + O_s^{2-} \xrightarrow{v_1'} h_s^+, \quad v_1' = k_1'[h_f^+][O_s^{2-}]$$

for non-protonated terminal oxygen ions and

$$h_f^+ + (O^{2-} - H^+)_s \xrightarrow{v_1'} h_s^+, \quad v_1' = k_1'[h_f^+][(O^{2-} - H^+)_s]$$

for protonated oxygen ions, where surface trapped holes should be identified with $(O^- - H^+)_s$ species.

Charge-carrier recombination

$$h_s^+ + e_f^- \xrightarrow{v_{r,1}'} O_s^{2-}, \quad v_{r,1}' = k_{r,1}'[e_f^-][h_s^+]$$

Interfacial-charge transfer

$$e_f^- + (O_2)_{aq} \xrightarrow{v_{red}'} O_2^-, \quad v_{red}' = k_{red}'[e_f^-][O_2]_{aq},$$

$$h_s^+ + (RH_2)_{aq} \xrightarrow{v_{ox}^{ind}} RH_{aq}^\bullet + H_{aq}^+, \quad v_{ox}^{ind} = k_{ox}^{ind}[h_s^+][RH_2]_{aq},$$

$$h_s^+ + RH_{aq}^\bullet \xrightarrow{v_{ox}^{ind,2}} R_{aq} + H_{aq}^+, \quad v_{ox}^{ind,2} = k_{ox}^{ind,2}[h_s^+][RH_{aq}^\bullet]$$

k_0' is an empirical proportional factor that depends on the nature of the catalyst, the reactor geometry and/or the film thickness if the semiconductor is immobilized as a nanoporous film [23]. If we assume that this factor does not depend on Φ, such a constant will not affect to the model predictions. On the other hand, TiO_2 is a semiconductor with an indirect optical transition; consequently, the recombination process will take place with participation of free electrons and surface trapped holes rather than via free electrons and free holes [8].

The back reaction $H_{aq}^+ + e_f^- + (RH_{aq}^\bullet) \xrightarrow{v_{back}^{ind}} (RH_2)_{aq}$ is not considered since, in practice, $k_{back}^{adb} \propto \exp[-(E_C - E_{ox})^2/4\lambda kT]$ must be very small compared with $k_{ox}^{ind} \propto \exp[-(E_{red} - E(h_s^+))^2/4\lambda kT]$, as $(E_C - E_{ox}) \gg (E_{red} - E(h_s^+))$ if an efficient photooxidation reaction is to be expected.

Under steady-state conditions the following expression is obtained for the IT quantum yield [12]

$$(QY)^{ind} = \left[\left(\frac{a[(RH_2)_{aq}]}{\Phi}\right)^2 + \frac{2a[(RH_2)_{aq}]}{\Phi}\right]^{1/2} - \frac{a[(RH_2)_{aq}]}{\Phi} \tag{3}$$

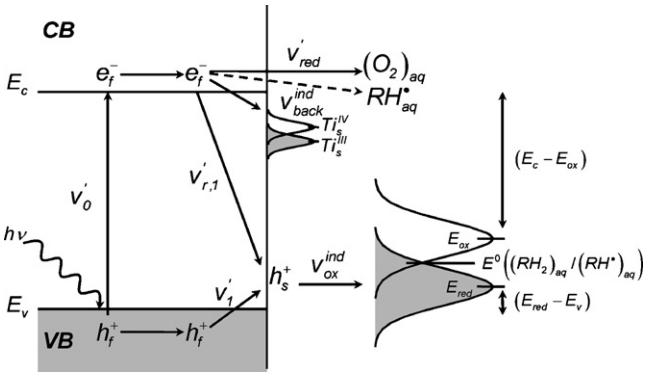

Fig. 3. Energy diagram showing the primary interfacial reactions involved in the indirect hole transfer mechanism.

with $a = k_{ox}^{ind} k'_{red}[O_2]/4k'_{r,1}k'_0$, which is a photon flux and reactant concentration independent constant. a is susceptible to be modified experimentally, allowing for the control of the quantum yield.

According to Eq. (3), an increase of the constant a leads to a QY increase. But a can be increased via an increase of k'_{red} and/or k_{ox}^{ind}, or a decrease of $k'_{r,1}$. Since $k'_{r,1}$ depends on the nature of the Ti–O chemical bonds in the TiO_2 structure, its modification is not easy. However, k'_{red} and k_{ox}^{ind} are both rate constants for the adiabatic charge transfer between energy levels of the semiconductor surface and dissolved reactant species of the electrolyte, and can be modified in a simpler way. For instance, the adsorption of inorganic anions (e.g., F^-) on the Ti surface atoms, which implicates desorption of adsorbed water species, produces a change of the TiO_2 net electric surface charge. This produces a shift of the semiconductor energy levels with respect to the electrolyte that leads to a change of the $(E_{red} - E(h_s^+))$ energy difference in Eq. (2). The consequence is a change of both k_{ox}^{adb} and k'_{red}, that leads to a modification of the QY [23]. This allows to explain in a simple way the observed increase of phenol photooxidation rate when the TiO_2 surface becomes fluorinated, without necessity of invoking the photogeneration of free OH radicals which, as shown in Section 2, is an unrealistic hypothesis.

Fig. 4 shows plots of $(QY)^{ind}$ versus Φ, $\log(QY)_{IT}$ versus $\log \Phi$ and $(QY)^{ind}$ versus $\Phi^{-1/2}$. The main features of Fig. 4 are: (1) the quantum yield increases steadily as Φ decreases (no maximum is predicted in the $(QY)^{ind}$ vs. $[(RH_2)_{aq}]$ plot); (2) $\lim_{\Phi \to 0} QY = 1$; (3) $(QY)^{ind} \propto \Phi^{-m}$, with $0 < m \leq 1/2$, and $m = 1/2$ for $\Phi/[(RH_2)_{aq}] \gg a/2$.

The IT quantum yield dependence on the substrate concentration for different Φ values is shown in Fig. 5. The main features in this case are: (1) the higher $[(RH_2)_{aq}]$, the lower $\partial(QY)^{ind}/\partial[(RH_2)_{aq}]$; (2) $1/((QY)^{ind})$ does not depend linearly on $1/[(RH_2)_{aq}]$ in the whole $[(RH_2)_{aq}]$ range (the LH model does not apply); (3) the $[(RH_2)_{aq}]$ range where linearity apparently exist increases as Φ decreases. The influence of the k_{ox}^{adb} rate constant on the QY has been analyzed in Ref. [12].

Kinetic expressions like that described by Eq. (3), where $QY \propto \Phi^{-1/2}$ for high enough illumination intensity values, have been obtained by Gerischer [3] and Minero et al. [24,25] by considering primary chemical reaction events similar to those used by us. Martyanov and Savinov [26] also obtain a similar expression by considering that the loss of activity of photoexcited TiO_2 particles takes place via $OH^\bullet$ radical combination ($OH^\bullet + OH^\bullet \rightarrow H_2O_2$), something kinetically improbable if compared with $OH^\bullet$ annihilation via recombination with free conduction band electrons. However, for these authors, the rate constants k_{ox}^{adb} and k_{red} did not have a specific physical meaning in contrast with the D–I model. This constitutes a serious limitation for predicting the actual behaviour of the photocatalytic system when experimental parameters are modified [27].

5.2. The DT mechanism

Since DT always coexists with IT, the following interfacial reactions should also be considered [12]:

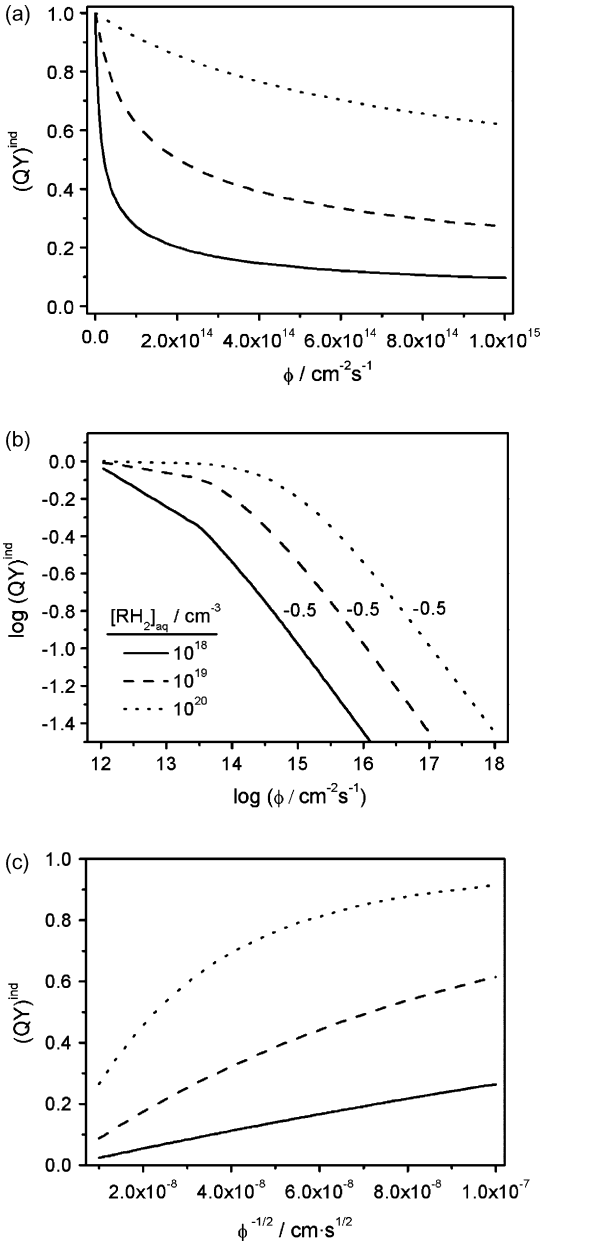

Fig. 4. Influence of the pollutant concentration on the IT quantum yield dependence on the illumination intensity (linear plot (a) and logarithmic plot (b)), and on the square root of the illumination intensity (c), according to Eq. (3). The following parameters were used: $k'_{red}[O_2] = 10^{-3}\ cm\ s^{-1}$, $k'_0 = 10^{-3}$, $k'_{r,1} = 10^{-8}\ cm^3\ s^{-1}$ and $k_{ox}^{ind} = 10^{-13}\ cm^3\ s^{-1}$). The slopes of $\log(QY)^{ind}$ vs. $\log \Phi$ are indicated in (b).

Interfacial-charge transfer

$$h_f^+ + (RH_2)_s \xrightarrow{v_{ox}^d} RH_s^\bullet + H_{aq}^+, \quad v_{ox}^d = k_{ox}^d [h_f^+][(RH_2)_s]$$

Back reactions

$$H_{aq}^+ + e_f^- + RH_s^\bullet \xrightarrow{v_{back}^d} (RH_2)_s, \quad v_{back}^d = k_{back}^d [e_f^-][RH_s^\bullet]$$

With respect to the adsorption/desorption kinetics of $(RH_2)_{aq}$ species, two different cases arise.

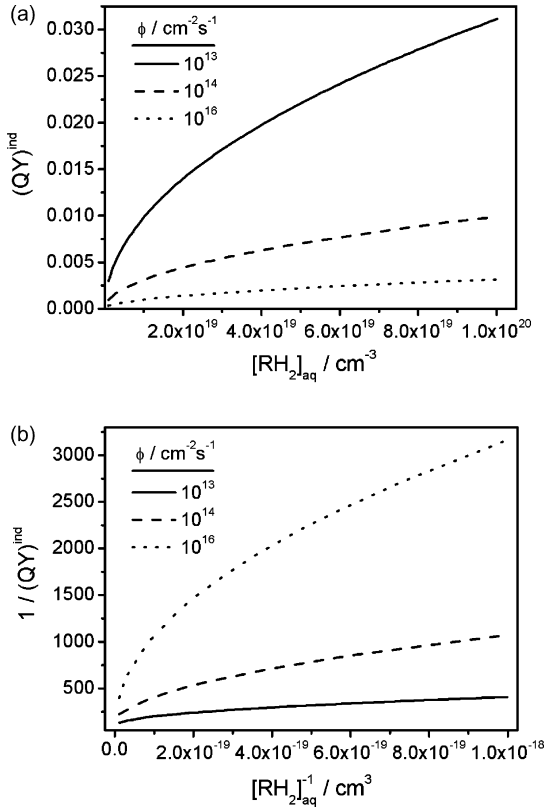

Fig. 5. Plots of: (a) quantum yield vs. pollutant concentration, (b) inverse of the IT quantum yield vs. the inverse of the pollutant concentration, for different illumination intensities, according to Eq. (3). The following parameters were used: $k'_{red}[O_2] = 10^{-3}\,cm\,s^{-1}$, $k'_0 = 10^{-3}$, $k'_{r,1} = 10^{-8}\,cm^3\,s^{-1}$, $k_{ox}^{ind} = 10^{-18}\,cm^3\,s^{-1}$.

5.2.1. *Equilibrated adsorption of reactants (the adsorption/desorption equilibrium in the dark is not modified under illumination)*

If a Langmuir type adsorption isotherm is assumed, the following relationship exists between the concentration of dissolved and adsorbed species

$$[(RH_2)_s] = \frac{ab[(RH_2)_{aq}]}{1 + a[(RH_2)_{aq}]} \tag{4}$$

where a is the adsorption constant and b is the density of surface sites available for adsorption. Therefore, the quantum yield for direct hole transfer becomes [12]:

$$\begin{aligned}(QY)^d &= \frac{v_{ox}^d + v_{ox}^{ind} - v_{back}^d}{v_0} \\ &= \frac{k_{ox}^d[(RH_2)_{aq}]ab}{(ak'_1[O_s^{2-}] + abk_{ox}^d)[(RH_2)_{aq}] + k'_1[O_s^{2-}]} \\ &\quad + \frac{k_{ox}^{ins}[O_s^{2-}][(RH_2)_{aq}]}{k'_0\Phi} \\ &\quad - \frac{k_{back}^d[(RH_s^\bullet)]}{k_{back}^d[(RH_s^\bullet)] + k'_{r,1}[h_s^+] + k'_{red}[O_2]}\end{aligned} \tag{5}$$

Fig. 6 shows the quantum yield dependence on the photon flux according to Eq. (5). It is inferred from this figure that for low enough Φ values the quantum yield is governed by an IT mechanism, while for high enough Φ values DT predominates on IT, the quantum yield becoming Φ independent. This behaviour is due to the absence of intermediary species (OH radicals in the IT mechanism) acting simultaneously as recombination and interfacial charge transfer centres in the DT mechanism. To our knowledge, no kinetic model has been proposed up to date predicting the behaviour of Eq. (5), i.e., the existence of a transit from a linear dependence of the QY on $\Phi^{1/2}$ for low enough Φ values to a photon flux independent QY for high enough Φ values. Eq. (5) also explains why under appropriated modification of the TiO_2 surface (e.g., by fluorination), so that specific adsorption of the reactant (e.g., formic acid) becomes hindered ($v_{ox}^d = 0$), a transit from DT to IT is produced and a quantum yield decrease is observed [27,28]. In contrast, in the absence of specific adsorption of the reactant (e.g., phenol), as surface fluorination produces an increase of the k_{ox}^{ind} rate constant, the QY increases [27]. Plots of $(QY)^d$ versus $[(RH_2)_{aq}]$, and $1/(QY)^d$ versus $1/[(RH_2)_{aq}]$ for variable photon flux, according to Eq. (5), are shown in Fig. 7. As can be seen, the higher $[(RH_2)_{aq}]$, the lower $d(QY)^d/d[RH_2]_{aq}$, the quantum yield becoming apparently flat for high enough Φ and $[(RH_2)_{aq}]$ values ($\Phi \geq 10^{15}\,cm^{-2}\,s^{-1}$ and $[(RH_2)_{aq}] \geq 10^{18}\,cm^{-3}$). Moreover, for high enough Φ values ($\Phi \geq 10^{12}\,cm^{-2}\,s^{-1}$), $1/(QY)^d$ depends linearly on $1/[(RH_2)_{aq}]$ (L–H behaviour), the linearity range increasing with Φ. The influence of the interfacial electron transfer rate constant and recombination rate constant on $(QY)^d$ has been analyzed in Ref. [12].

Studying the photooxidation of formic acid, which adsorbs specifically on TiO_2 [27], Dijkstra et al. [29] found a photon flux independent QY, as predicted by the DT mechanism. In fact, a similitude exists between Eqs. (5) and (16) of Ref. [29]. These authors attribute formic acid degradation to the reaction of free holes or adsorbed, photogenerated OH radicals with specifically adsorbed reactant molecules [29]. Interestingly, Dijkstra et al. propose a reactions scheme that omits photogenerated intermediate radicals acting simultaneously as recombination and interfacial electron transfer centres, as assumed by our DT mechanism.

5.2.2. *Non-equilibrated adsorption of reactants (the adsorption/desorption equilibrium in the dark is broken under illumination)*

The L–H model assumes equilibrated adsorption of reactants. According to Ollis [9], this is the reason why frequently the L–H model is not able to fit the kinetics of the catalyzed photooxidation reactions. For instance, Emeline et al. found that experimental kinetics concerning phenol photooxidation is apparently fitted by the L–H model [11], although they arrive to the internal contradiction that the K_L Langmuir constant is photon flux dependent. In order to overcome this drawback, Ollis assumes that adsorption–desorption equilibrium is broken under illumination conditions and proposes a pseudo-steady-state analysis for reaction intermediates [9]. Ollis arrives to the following expression for the photooxidation rate (r): $r = k_{cat}^{app}k_{diss}^{app}C_A/(k_{diss}^{app} + C_A)$,

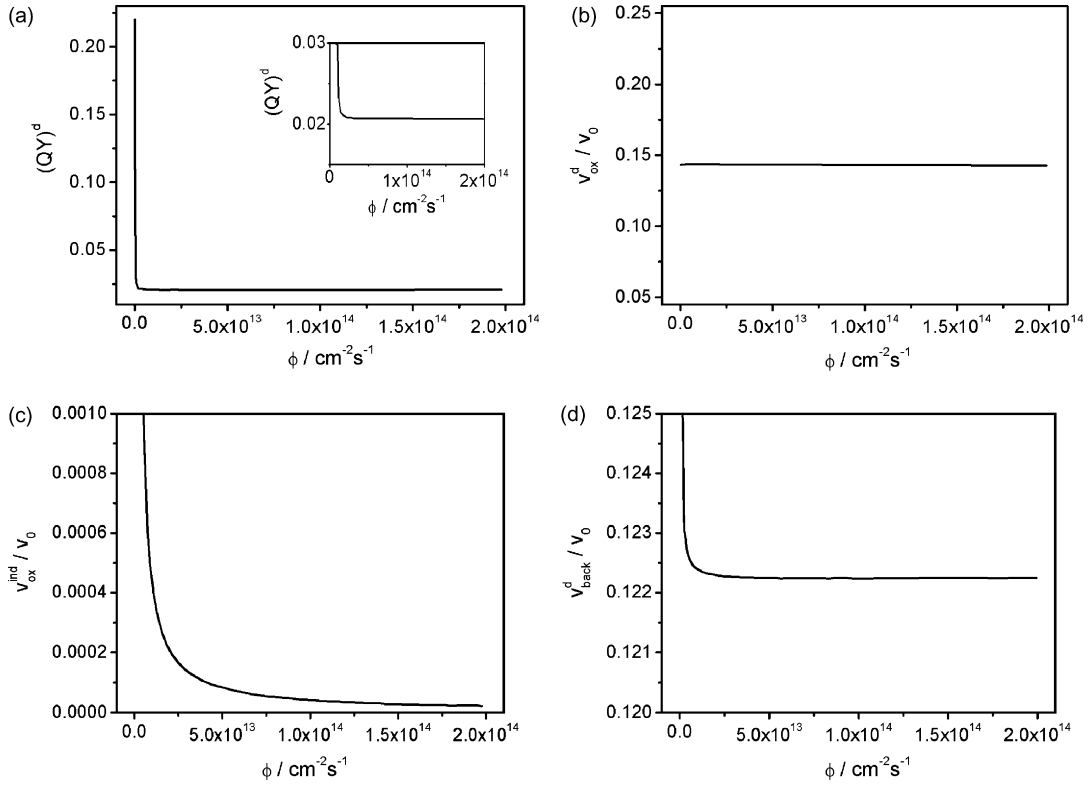

Fig. 6. (a) Quantum yield vs. illumination intensity plots according to Eq. (5). The influence of direct hole transfer, indirect hole transfer and recombination via $RH_s^{\bullet}$ intermediate species to the global quantum yield, $(QY)_{DT}$, is shown in (b), (c) and (d), respectively. The following parameters were used: ($k'_{red}[O_2] = 10^{-3}$ cm s^{-1}, $k'_0 = 10^{-3}$, $a = 10^{-18}$ cm^{-3}, $b = 10^{14}$ cm^{-2}, $k'_1 = k^d_{ox} = k'_{r,1} = k^d_{back} = 10^{-8}$ cm^3 s^{-1}, $[O_s{}^{2-}]_{in} = 3 \times 10^{14}$ cm^{-2}, $[(RH_2)_{aq}] = 10^{18}$ cm^{-3}).

where C_A is the substrate concentration, while k^{app}_{cat} and k^{app}_{diss} are photon-flux-dependent, apparent rate constant and the dissociation constant, respectively. Apparently, Ollis' model is able to save the internal contradiction found by Emeline et al. when analyzing phenol photooxidation experimental data with the L–H model [11]. However, Ollis' model assumes that the photocatalytically active surface species are OH radicals, either adsorbed or dissolved (free), generated by the photooxidation of adsorbed water species with valence band holes [4,9], which, as shown in Section 2, is questionable. In the following we will apply Ollis' idea of non-equilibrated adsorption of reactants to the case where photocatalytically active species are not OH radicals but photogenerated valence band free holes able to attack specifically adsorbed species via an inelastic DT mechanism.

Table 2
Experimental tests for differentiating direct from indirect interfacial hole transfer according to the D–I kinetic model

Substrate–TiO_2 interaction	Adsorption site	Predominant interfacial charge transfer mechanism	Kinetics dependence on illumination flux (Φ) and substrate concentration ($[RH_2]_{aq}$)
Weak (non-specific adsorption)		IT at any Φ	$\Phi \to 0 \begin{cases} QY \to 1 \\ Rate \to 0 \end{cases}, \frac{\Phi}{[RH_2]_{aq}} \gg \frac{k'_{ox}k_{red}[O_2]}{8k'_{r,1}k'_0} \begin{cases} QY \propto \Phi^{-1/2}[RH_2]^{1/2}_{aq} \\ QY \propto \Phi^{1/2}[RH_2]^{1/2}_{aq} \end{cases}$, $\frac{1}{QY}$ vs. $\frac{1}{[RH_2]_{aq}}$, non-linear
Strong (specific adsorption)			
(a)Equilibrated adsorption of reactants	Terminal Ti^{IV}_s	IT at small enough Φ; DT at high enough Φ	$\begin{matrix} QY = const \\ Rate \propto \Phi \end{matrix}$ $\frac{1}{QY} \propto \frac{1}{[RH_2]_{aq}}$, $\lim_{[RH_2]_{aq}\to\infty} \left\{ \begin{matrix} QY^{-1} \\ Rate^{-1} \end{matrix} \right\}$ vs. $[RH_2]^{-q}_{aq}$ $\begin{matrix} Const. \\ Const./\Phi \end{matrix}$
	Terminal $O_s{}^{2-}$	DT at any Φ	$\begin{matrix} QY = const \\ Rate \propto \Phi \end{matrix}$, $\frac{1}{QY}$ vs. $\frac{1}{[RH_2]_{aq}}$, linear
(b) Non-equilibrated adsorption of reactants	Terminal Ti^{IV}_s	IT at small enough Φ; DT at high enough Φ	Rate vs. and $\frac{1}{QY}\frac{1}{[RH_2]_{aq}}$ non-linear
	Terminal $O_s{}^{2-}$	DT at any Φ	$\begin{matrix} QY = const \\ Rate \propto \Phi \end{matrix}$, $\frac{1}{QY}$ vs. $\frac{1}{[RH_2]_{aq}}$, linear

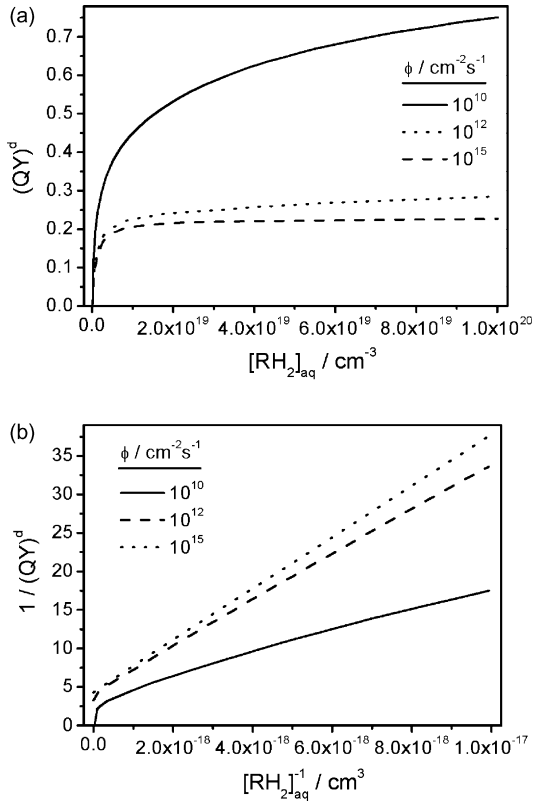

Fig. 7. Influence of the illumination intensity on the dependence of: (a) quantum yield on the pollutant concentration, (b) inverse of the quantum yield on the inverse of the pollutant concentration, according to Eq. (5). The following parameters were used: $k_{ox}^{ind} = 10^{-18}\,cm^3\,s^{-1}$, $k'_{red}[O_2] = 10^{-3}\,cm\,s^{-1}$, $k'_0 = 10^{-3}$, $a = 10^{-18}\,cm^{-3}$, $b = 10^{14}\,cm^{-2}$, $k'_1 = k_{ox}^{d} = k'_{r,1} = 10^{-8}\,cm^3\,s^{-1}$, $[O_s^{2-}]_{in} = 3 \times 10^{14}\,cm^{-2}$, $k_{back}^{d} = 10^{-8}\,cm^3\,s^{-1}$.

According to the pseudo-steady-state approach proposed by Ollis [9], it can be written for DT:

$$\frac{d\theta_A}{dt} = [RH_2]_{aq} k_1 (1 - \theta_A) - k_{-1}\theta_A - k_{ox}^{d}[h_f^+]\theta_A = 0 \quad (6)$$

where k_1 and k_{-1} are the adsorption and desorption constant, respectively ($k_1/k_{-1} = a$ in Eq. (4)), so that it becomes:

$$[(RH_2)_s] = \frac{ab[(RH_2)_{aq}]}{1 + a[(RH_2)_{aq}] + ((k_{ox}^{d}/k_{-1})(k'_0\Phi/(k_1[O_s^{2-}] + k_{ox}^{d}[(RH_2)_s]))} \quad (7)$$

In contrast with Eq. (4), Eq. (7) shows that $[(RH_2)_s]$ decreases as Φ increases. Moreover, under steady-state conditions it can be written

$$\frac{d[h_f^+]}{dt} = v'_0 - v'_1 - v_{ox}^{d} = 0 \quad (8)$$

$$\frac{d[e_f^+]}{dt} = v'_0 - v'_{r,1} - v'_{red} - v_{back}^{d} = 0 \quad (9)$$

$$\frac{d[h_s^+]}{dt} = v'_1 - v_{ox}^{ind} - v'_{r,1} = 0 \quad (10)$$

$$\frac{d[(RH_2)_s]}{dt} = v_{ox}^{d} - v_{back}^{d} = 0 \quad (11)$$

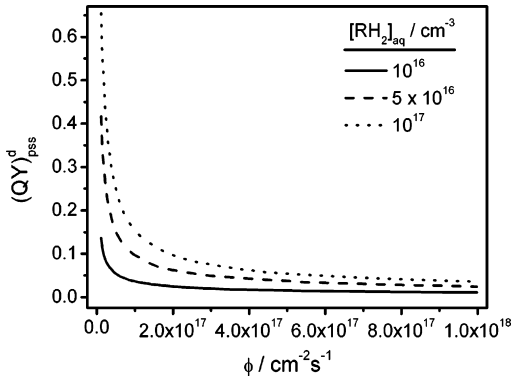

Fig. 8. Plot of the photooxidation quantum yield vs. photon flux, for variable concentration of $(RH_2)_{aq}$ dissolved species, according to the pseudo-steady-state approach (adsorption/desorption equilibrium in the dark is broken under illumination), for direct interfacial hole transfer. The following parameters were used: $k_{ox}^{ind} = 10^{-10}\,cm^3\,s^{-1}$, $k_{ox}^{ins} = 10^{-6}\,cm^3\,s^{-1}$, $[O_s^{2-}]_{in} = 3 \times 10^{14}\,cm^{-2}$, $k_1 = 1\,s^{-1}$.

Fig. 8 shows the quantum yield dependence on the photon flux, for variable substrate concentration, under non-equilibrated adsorption of reactants, as defined by Eq. (5), obtained by solving numerically the system of Eqs. (7)–(11). Observe the analogy with the behaviour shown in Fig. 4(a) for IT, which

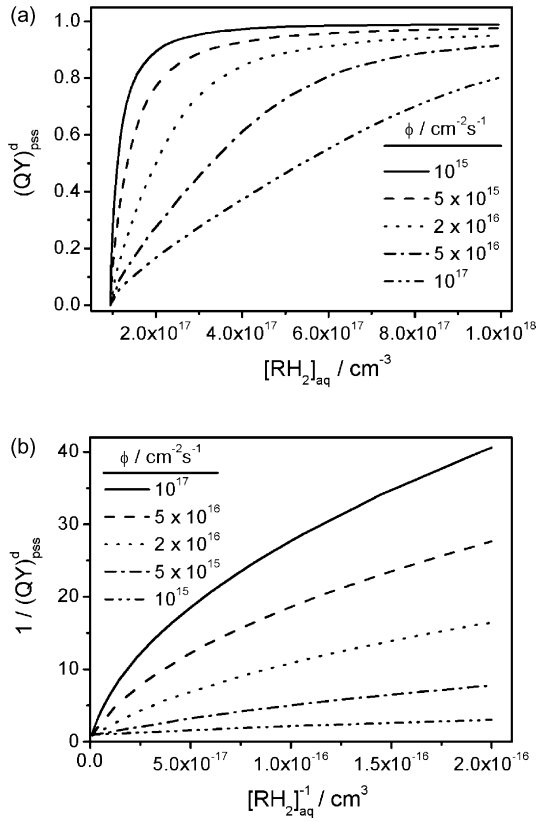

Fig. 9. Plots of: (a) direct quantum yield ($(QY)'_{DT}$) vs. concentration of $(RH_2)_{aq}$ dissolved species; (b) inverse of the quantum yield vs. the inverse of the concentration of dissolved species, according to the pseudo-steady-state approach (adsorption/desorption equilibrium in the dark is broken under illumination), for direct interfacial hole transfer. The following parameters were used: $k_{ox}^{ind} = 10^{-10}\,cm^3\,s^{-1}$, $k_{ox}^{d} = 10^{-6}\,cm^3\,s^{-1}$, $k'_{red}[O_2] = 10^{-3}\,cm\,s^{-1}$, $k'_0 = 10^{-3}$, $a = 10^{-18}\,cm^{-3}$, $b = 10^{14}\,cm^{-2}$, $k'_1 = k'_{r,1} = 10^{-8}\,cm^3\,s^{-1}$, $[O_s^{2-}]_{in} = 3 \times 10^{14}\,cm^{-2}$, $k_1 = 1\,s^{-1}$.

indicates that, in principle, it is difficult to distinguish between IT and DT in the absence of equilibrated adsorption/desorption. However, Fig. 9 shows the plots of the quantum yield versus the substrate concentration and the inverse of the quantum yield versus the inverse of substrate concentration, for different photon fluxes, obtained as for Fig. 8. Note that for low enough photon flux ($\Phi \leq 10^{15}$ cm^{-2} s^{-1}), when adsorption equilibrium becomes reestablished, the plot becomes linear. This feature allows to differentiate DT for non-equilibrated adsorption–desorption of reactants from IT, as in the first case linearity of $1/(\mathrm{QY})^{\mathrm{d}}_{\mathrm{pss}}$ versus $1/[(\mathrm{RH}_2)_{\mathrm{aq}}]$ is never reached for low Φ values.

Experimental tests for differentiating DT and IT mechanisms from the quantum yield dependence on photon flux and substrate concentration are summarized in Table 2. Literature examples where the QY is found to depend linearly on $\Phi^{-1/2}$, as corresponds to IT, are those concerning photooxidation of methanol [30,31], chloroform [32], methylviologen [26], 2-propanol [33] and phenol [34]. On the other hand, the photooxidation of formic acid [29], and acetic acid [35], are examples of DT, as a photon flux independent quantum yield has been reported.

Acknowledgements

Financial support from the Ministerio de Educación y Ciencia (MEC) through projects BQU2003-03737, CTQ2006-06286/BQU (Fondos FEDER) and TIN2004-07926-E, and from the Generalitat Valenciana through project GV05-119, is greatly acknowledged. D.M.S. is also grateful to the MEC (Spain) for the award of a FPI grant.

References

[1] As obtained from SciFinder Scholar™ 2006, The American Chemical Society.
[2] C. Kormann, D.W. Bahnemann, M.R. Hoffmann, N.S. Lewis, J. Phys. Chem. 98 (1994) 13385.
[3] H. Gerischer, Electrochim. Acta 40 (1995) 1277.
[4] C.S. Turchi, D.F. Ollis, J. Catal. 122 (1990) 178.
[5] C. Minero, G. Mariella, V. Maurino, E. Pelizzetti, Langmuir 16 (2000) 2632.
[6] J. Cuningham, G. Al-Sayed, S. Srijaramai, in: G. Gels, R.G. Zeep, D.G. Grosby (Eds.), Aquatic and Surface Photochemistry, Lewis, Boca Raton, FL, 1994, pp. 317–348.
[7] M.A. Fox, M.T. Dulay, Chem. Rev. 93 (1993) 341.
[8] M.R. Hoffmann, S.T. Martin, W. Choi, D.W. Bahnemann, Chem. Rev. 95 (1995) 69.
[9] D.F. Ollis, J. Phys. Chem. B 109 (2005) 2439.
[10] A.V. Emeline, V.K. Ryabchuck, N. Serpone, J. Phys. Chem. B 109 (2005) 18515.
[11] A.V. Emeline, V.K. Ryabchuck, N. Serpone, J. Photochem. Photobiol. A: Chem. 133 (2000) 89.
[12] T. Lana-Villarreal, R. Gómez, M. González, P. Salvador, J. Phys. Chem. B 108 (2004) 20278.
[13] T. Lana-Villarreal, R. Gómez, M. Neumann-Spallart, N. Alonso-Vante, P. Salvador, J. Phys. Chem. B 108 (2004) 15172.
[14] I. Mora-Seró, T. Lana-Villarreal, J. Bisquert, A. Pitarch, R. Gómez, P. Salvador, J. Phys. Chem. B 109 (2005) 3371.
[15] R. Nakamura, Y. Nakato, J. Am. Chem. Soc. 126 (2004) 1290.
[16] P. Salvador, J. Phys. Chem. B, submitted for publication.
[17] D.W. Bahnemann, M. Hilgendorff, R. Memming, J. Phys. Chem. B 101 (1997) 4265.
[18] R.H. Marcus, J. Chem. Phys. 24 (1956) 966.
[19] H. Gerischer, Surf. Sci. 18 (1969) 97.
[20] H. Gerischer, in: P. Delahay (Ed.), Advances in Electrochemistry and Electrochemical Engineering, vol. I, Interscience, New York, 1961, p. 139.
[21] E. Pelizzetti, C. Minero, Electrochim. Acta 38 (1993) 47.
[22] S.R. Morrison, Electrochemistry at Semiconductors and Oxidized Metal Electrodes, Plenum Press, New York, 1980.
[23] C. Minero, D. Vione, Appl. Catal. B: Environ. 67 (2006) 257.
[24] C. Minero, Catal. Today 54 (1999) 205.
[25] C. Minero, V. Maurino, E. Pelizzetti, in: V. Ramamurthy, K.S. Schanze (Eds.), Semiconductor Photophysics and Photochemistry, Marcel Dekker, 2003.
[26] I.N. Martyanov, E.N. Savinov, J. Photochem. Photobiol. A: Chem. 134 (2000) 219.
[27] D. Monllor-Satoca, A. Rodes, R. Gómez, P. Salvador, J. Phys. Chem., submitted for publication.
[28] J.S. Park, W. Choi, Langmuir 20 (2004) 11523.
[29] M.F.J. Dijkstra, H.J. Panneman, J.G.M. Winkelman, J.J. Kelly, A.A.C.M. Beenackers, Chem. Eng. Sci. 57 (2002) 4895.
[30] C.-Y. Wang, J. Rabani, D.W. Bahnemann, J.K. Dohrmann, J. Photochem. Photobiol. A: Chem. 148 (2002) 169.
[31] C. Wang, D.W. Bahnemann, J.K. Dohrmann, Wat. Sci. Technol. 44 (2001) 279.
[32] C. Kormann, D.W. Bahnemann, M.R. Hoffmann, Environ. Sci. Technol. 25 (1991) 494.
[33] T.A. Egerton, C.J. King, J. Oil Colour Chem. Asoc. 62 (1979) 386.
[34] M. González-Hidalgo, P. Salvador, in preparation.
[35] M. Bideau, B. Claudel, L. Faure, H. Kazovan, J. Photochem. Photobiol. A: Chem. 61 (1991) 269.